



Fast-Response and Flexible Nanocrystal-Based Humidity Sensor for Monitoring Human Respiration and Water Evaporation on Skin

Kano, Shinya
Kim, Kwangsoo
Fujii, Minoru

(Citation)

ACS Sensors, 2(6):828-833

(Issue Date)

2017-06

(Resource Type)

journal article

(Version)

Accepted Manuscript

(Rights)

This document is the Accepted Manuscript version of a Published Work that appeared in final form in ACS Sensors, copyright © American Chemical Society after peer review and technical editing by the publisher. To access the final edited and published work see <http://dx.doi.org/10.1021/acssensors.7b00199>

(URL)

<https://hdl.handle.net/20.500.14094/90004879>



Fast-response and flexible nanocrystal-based humidity sensor for monitoring human respiration and water evaporation on skin

Shinya Kano, Kwangsoo Kim, Minoru Fujii*

Department of Electrical and Electronic Engineering, Graduate School of Engineering, Kobe University, Rokkodai, Nada, Kobe 657-8501, Japan

KEYWORDS

Humidity sensor, Silicon nanocrystal, Nanocrystal thin film, Flexible device, Health monitoring

ABSTRACT

We develop a fast-response and flexible nanocrystal-based humidity sensor for real-time monitoring human activity: respiration and water evaporation on skin. A silicon-nanocrystal film is formed on a polyimide film by spin-coating the colloidal solution and is used as a flexible and humidity-sensitive material in a humidity sensor. The flexible nanocrystal-based humidity sensor shows a high sensitivity; current through the nanocrystal film changes by five orders of magnitude in the relative humidity range of 8 – 83 %. The response/recovery time of the sensor is 40 ms. Thanks to the fast response and recovery time, the sensor can monitor

human respiration and water evaporation on skin in real time. Due to the flexibility and the fast response/recovery time, the sensor is promising for application in personal health monitoring as well as environmental monitoring.

Monitoring humidity in air is indispensable for modern industry, agriculture, and medical care.¹⁻³ Especially, real-time monitoring of humidity from human body becomes more important recently in the field of personal health monitoring.^{4,5} Mogera et al. proposed that dehydration of human body was detected from the analysis of humidity in human breath.⁶ Miyoshi et al. suggested non-invasive detection of physiological stress to human by monitoring sweat produced from sweat glands on fingers.⁷

Fast response and recovery are prerequisite features to apply humidity sensors for personal health monitoring. For respiratory and epidermal medical sensing, a flexible and wearable sensor is desirable because it can be fit directly to human skin.⁸ Flexible humidity sensors have been fabricated by depositing a humidity-sensitive film on a polymer substrate.⁷⁻¹³ As a fast-response humidity-sensitive film, various nanomaterials, such as porous materials^{14,15}, graphene-related materials^{11,13,16-18}, and organic polymers^{6,18}, have been recently investigated.

Colloidal quantum dot thin films, which can be prepared on flexible substrates by depositing the colloidal solution at low temperature, are promising candidates for flexible gas-sensitive materials.¹⁹ Because of the large surface-to-volume ratio, electrical characteristics of the film strongly depend on adsorbed molecules on the surface. Gas sensing by using quantum-dot thin films has been reported.^{12,20-24} Liu et al. proposed that highly size-regulated quantum dots can be a sensing material for a high-performance gas sensor: fast response, high sensitivity, and good reversibility.²³ Segev-Bar et al. have reviewed state-of-the-art flexible sensors based on quantum dots for smart sensing applications.¹⁹ Inspired by these works, we apply a colloidal quantum-dot film to a flexible humidity sensor. Among many kinds of colloidal quantum dots, colloidal silicon nanocrystals (Si NCs) are suitable for a wearable humidity sensor because of the high compatibility with conventional semiconductor processes and the nontoxicity to human body.²⁵⁻²⁷ Furthermore, surface-oxidized silicon is stable against volatile organic

compound gas from human body, which degrades the performance of commercial humidity sensors using organic polymers.

In this work, we employ all-inorganic colloidal Si NCs developed in our group as a precursor for the formation of a humidity-sensitive thin film.²⁶ The all-inorganic Si NCs have a heavily boron and phosphorus-codoped surface layer, which induces negative potential on the surface and makes the NCs hydrophilic.^{28–31} As a result, the Si NCs are dispersible in polar solvents such as alcohol and water without organic ligands.³² Because of the perfect dispersion in solution, a transparent and flexible NC thin film can be prepared by spin-coating. In our previous work, we studied the current transport property of the film in different atmosphere and obtained clear evidence that the film was very sensitive to the amount of water molecules in atmosphere.³³ In this study, we produce a flexible humidity sensor on a polymer substrate by using the all-inorganic colloidal Si NCs. We demonstrate that the response/recovery speed of the sensor is very fast and it can dynamically monitor human respiration and water evaporation on skin.

EXPERIMENTAL SECTION

Fabrication of NC-based humidity sensor. All-inorganic Si NCs were prepared using a co-sputtering method described in previous papers.^{26,28,32} Si-rich borophosphosilicate films were deposited on a stainless steel plate by co-sputtering Si, B₂O₃, and phosphosilicate glass (P₂O₅:SiO₂=5:95 wt%). The powder made from the deposited film was annealed in a N₂ atmosphere at 1200°C for 30 min to grow Si NCs about 7 nm in diameter. The Si NCs were extracted from SiO₂ matrices by hydrofluoric acid (46 wt%) etching. The Si NCs in hydrofluoric acid solution were transferred into methanol by centrifugation. Concentration of colloidal Si NCs in methanol was 0.5 mg/ml. Just after preparation, the surface of Si NCs is hydrogen-terminated and it is gradually oxidized during storage in methanol. In this work, we used Si NCs stored in methanol for more than 60 days and the thickness of the surface oxide is around 1 nm.²⁹

The fabrication process of a NC thin-film humidity sensor is as follows. Titanium and gold interdigitated electrodes were fabricated by thermal evaporation with a metal mask on a fused silica substrate or a 25- μ m thick polyimide film. The thicknesses of titanium and gold were 7 and 63 nm, respectively, on a fused silica substrate, and 6 and 66 nm, respectively, on a polyimide film. The width, separation, and overlap of the interdigitated electrodes were 100 μ m, 100 μ m, and 4 mm, respectively. The number of electrode pairs was 10. Colloidal Si-NC solution was spin-coated on the substrate cleaned by ultrasonication in alcohol (acetone and isopropyl alcohol) and UV/O₃ treatment. Spin-coating condition was 500 rpm for 5 sec, followed by 2000 rpm for 60 sec. Figure 1(a) is the schematic illustration of a finished NC-based sensor. Note that the Si-NC thin film is not intentionally sintered, and thus the NC film behaves as an insulator rather than a semiconductor due to the surface oxide.³⁴

Figure 1(b) shows the picture of NC-based humidity sensors on a fused silica substrate. The NC thin film over the interdigitated electrodes is transparent. No large agglomeration of the NCs is observed by using an optical microscope (Figure 1(c)). Figure 1(d) shows the topographic image of the NC film between the interdigitated electrodes by atomic force microscopy (HITACHI High-Tech Science, SPA-400). The image is visualized by using Gwyddion.³⁵ This image ensures that a dense Si-NC thin film is formed by spin-coating. The surface roughness is 3.3 nm in $2\ \mu\text{m} \times 2\ \mu\text{m}$. The size of agglomerates on the film is smaller than 50 nm from the image, which coincides with the high transparency of the NC film in Figure 1(b).

Measurement setup. The sensing property of a NC-based humidity sensor was measured in a homemade box. Humidity in the box was controlled by N₂ carrier gas with bubbling distilled water. Current through the film was measured by a source measure unit (Keithley, 236) or a combination of a current amplifier (Keithley, 428) and a digital oscilloscope (Iwatsu, DS-5634A). Silver paste and gold wires were used to have electrical contacts on the sensor. Relative humidity in the box was simultaneously recorded by using a commercial humidity sensor (TDK, CHS-UGS). The accuracy of the commercial sensor was $\pm 5\%$ of relative humidity. In a bending experiment, the sensor on a polyimide film was rolled around a glass bottle with a 5-mm radius of curvature (R). The sensor was fixed by using a double-sided tape on the glass bottle.

Evaluation of response speed was carried out by using a mechanical chopper and humid N₂ gas. Humid N₂ gas was chopped and modulated current through the sensor was detected by using a lock-in amplifier (Stanford Research System, SR830) and a function generator (NF, WF1947) as shown later. In the experiments of real-time monitoring human respiration and water evaporation on skin, the sensor was under ambient condition with relative humidity

around 20—40 %. Current response of the sensor was recorded by the digital oscilloscope after amplification by the current amplifier.

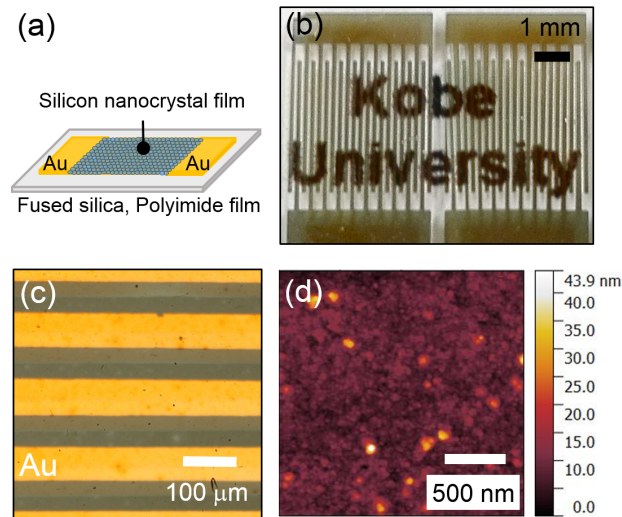


Figure 1. (a) Schematic illustration of a NC-based humidity sensor. (b) Whole picture and (c) optical microscope image of NC-based humidity sensors on a fused silica substrate. (d) Topographic image of the NC film.

RESULTS AND DISCUSSION

Sensing humidity by NC-based humidity sensor. Figure 2(a) shows bent interdigitated electrodes on a polyimide film. Gold/titanium interdigitated electrodes are strong enough for bending experiments. A flexible NC-based humidity sensor can be rolled up. Figure 2(b) shows a humidity sensor rolled up on a glass bottle with $R=5$ mm. Figure 2(c) shows the current readout of the NC-based humidity sensor as a function of relative humidity. In these measurements, 5 V was applied to the sensor at room temperature ($\sim 20^{\circ}\text{C}$). The data of the flat and bent sensors are shown. The current through the sensor increases by five orders of magnitude as the relative humidity in the box increases. The sensor detects 8 – 83 % of relative humidity and hysteresis of the readout is negligibly small, which is important for gas sensors.³ The sensing property is identical between flat and bent sensors. Regarding current-voltage characteristics of the NC-based sensor, Ohmic behavior is observed in both flat and bent conditions (Figure S-1 in Supporting Information). It should be stressed here that no notable current change is observed for interdigitated electrodes if a Si-NC film is not formed (~ 100 pA at 85 % relative humidity in Figure S-2 in Supporting Information).

Figure 2(d) shows a schematic illustration of the mechanism of carrier transport on the Si-NC film. The conduction is considered to be dominated by Grotthuss mechanism^{1,36} and proton transport occurs in water layers as reported in silica gels³⁷ and oxidized Si surface³⁸. In this model, when a physisorbed water-molecule layer is formed, protons are moved by an electric field through hydrogen-bonded water molecules via hopping. Therefore, the conductance of an insulative NC film depends on the amount of water molecules on the NC surface. The fact that the current-voltage characteristics, i.e., the Ohmic behavior, does not change under bending indicates that water layers are uniformly formed between gold electrodes without any breakage, because a breakage behaves as a tunneling barrier and makes the current-voltage characteristics

nonlinear. We believe that the space between NCs is covered with water layers uniformly as shown in Figure 2(d), which can be sustained even when the sensor is bent. The proton transfer occurs through the top of the water layers, and therefore, the increase of current is saturated when the surface of NC films is completely covered by water molecules. This explains the saturation behavior of the current in Figure 2(c) at high humid levels ($>70\%$).

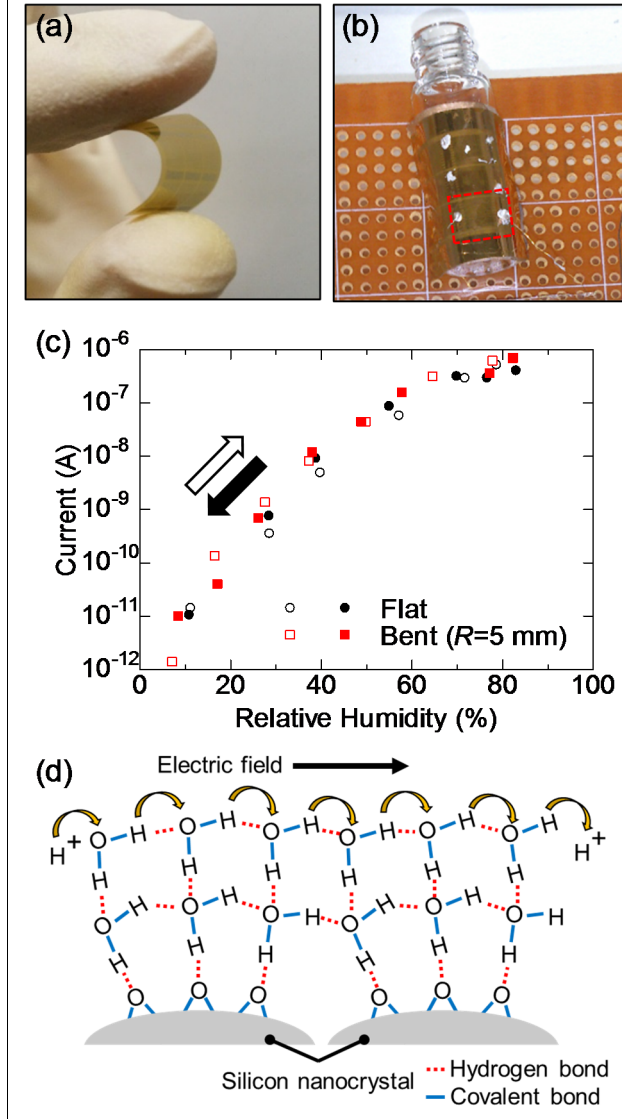


Figure 2. (a) Bent interdigitated electrodes on a polyimide film. (b) A bent NC-based humidity sensor on a glass bottle with $R=5$ mm. The measured device is indicated by a dashed square. (c) Current readout of the NC-based humidity sensor as a function of relative humidity. Open and filled marks represent measurements increasing and decreasing humidity, respectively. The bent sensor in Figure 2(b) was used in this measurement. (d) Schematic illustration of carrier transport on Si-NC surface.

Response and recovery time. Response/recovery speed of humidity sensors is essential for real-time monitoring of human activity. Figure 3(a) shows the measurement system for the evaluation of response/recovery speed. The chopped humid N₂ gas is blown on a NC-based sensor in the atmosphere (relative humidity: ~20 %). The change of current is detected by a lock-in measurement (current gain: 10^6) with an applied voltage of 5 V_{p-p} at 150 Hz. The humid

N₂ gas blow changes the local relative humidity about 10% according to the signal of the humidity sensor (Figure S-3(a) in Supporting Information) and the humidity dependence in Figure 2(c). The current responses at different frequencies are shown in Figure 3(b). The current response in the 3-Hz modulation is rectangular. The response becomes weak as the frequency increases. The modulated current can be observed up to 24 Hz. We also confirm that the response disappears when the humid N₂ gas flow is stopped.

The response (recovery) time of humidity sensors is defined as the time to achieve 90 % of total change from low to high (from high to low) humidity.^{3,14,39,40} According to this definition, the sensor response and recovery time in the 3-Hz modulation is 40 ms. This speed is enough for monitoring human activity such as respiration and motion of body. Table 1 lists response and recovery time of flexible humidity sensors for monitoring human respiration reported recently. Our NC-based humidity sensor is as fast as the ultrafast humidity sensor using graphene oxide (~30 ms)¹³. Although the response is not saturated above 9 Hz, the sensor can provide a trigger signal of quick change of humidity to external circuits up to 24 Hz.

We also evaluate the response and recovery time when humidity changes abruptly from 20 and 95 % and vice versa. They are 12 s and 3 s, respectively (Figure S-4 in Supporting Information). These values are shorter than those of resistive-type commercial humidity sensors using organic polymers. The shorter time for the recovery than for the response may be explained by the convex surface of NC films, which enhances desorption of water molecules according to the Young-Laplace equation in spherical form⁴¹: $\Delta P = 2\sigma/R$, where ΔP is the pressure difference across air-liquid interface, σ is the surface tension. We carried out an experiment to study temperature dependence of the humidity sensor response. The sensor showed smaller response as the temperature was raised because the intensity of current of the

sensor decreased. By now, it is difficult to evaluate response speed of the sensor at higher temperature.

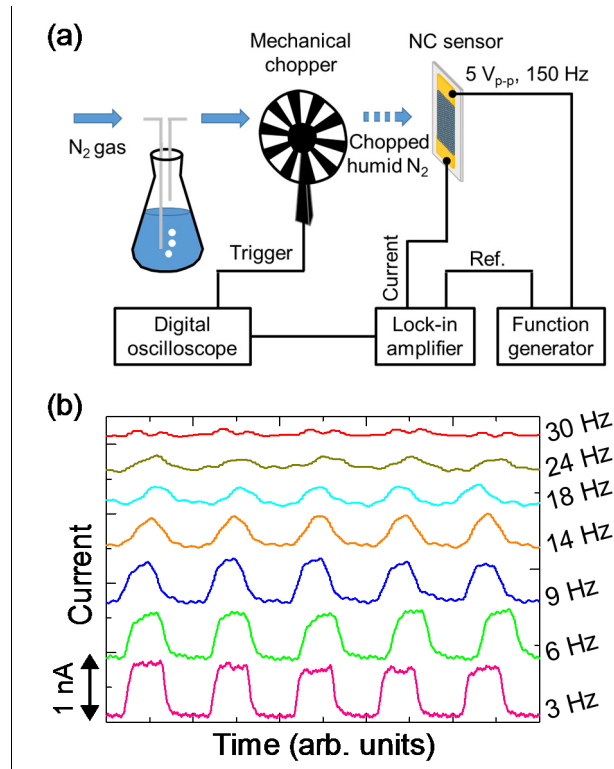


Figure 3. (a) Measurement system for evaluation of response speed. (b) Current response of a NC-based humidity sensor to chopped humid N₂ gas.

Table 1. Response and recovery time of flexible humidity sensors for monitoring human respiration in recent literature.

Humidity-sensitive material	Sensor type	Response time (s)	Recovery time (s)	Reference
Hydrophilic poly-tetrafluoroethylene membrane	Resistive	1	1	Y Miyoshi, et al. ⁷
Bis(benzo cyclobutene)	Capacitive	216	N/A	E. Zampetti, et al. ⁴²
Graphene oxide	Impedance	0.03	0.03	S. Borini, et al. ¹³
Graphene oxide/polyelectrolyte nanocomposite	Capacitive	1	1	D. Zhang, et al. ¹⁸
Cellulose paper	Resistive	1500	N/A	F. Guder, et al. ⁴³
Silicon-nanocrystal film	Resistive	0.04	0.04	This work

Monitoring human respiration. We demonstrate two possible applications of the fast-response humidity sensor for health monitoring: real-time detection of human respiration and water evaporation on skin. Figure 4(a) shows the measurement system for monitoring human respiration. The sensor is attached on a hand and exposed to human respiration. The distance between the sensor and the mouth is approximately 20 cm. Breath from the mouth is given to the sensor intermittently. Figure 4(b) is the demonstration of monitoring human respiration by the NC-based humidity sensor. Human breath can be detected as a sharp increase of current intensity. The relative humidity around the sensor changes locally by around 10% due to breath. The sensor can follow 1-sec interval of respiration. No notable decrease of the signal is observed during the human respiration tests, and thus the NC-based humidity sensor can be used for monitoring human respiration.

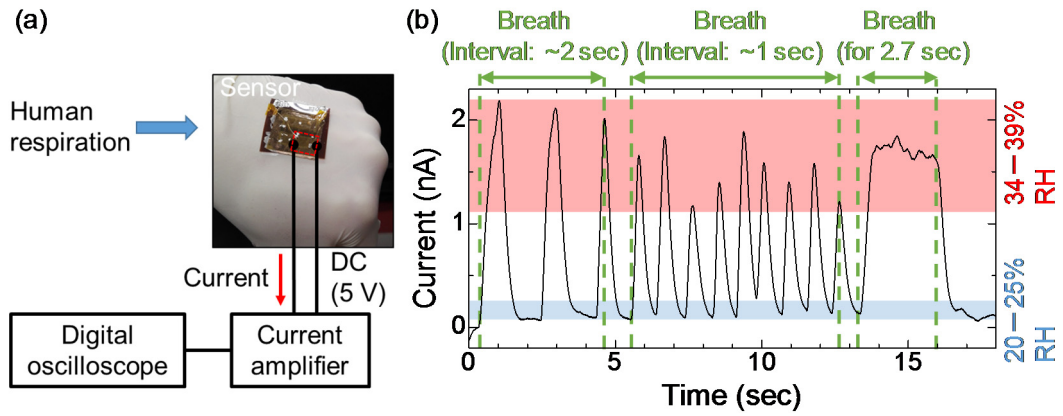


Figure 4. (a) Measurement system for monitoring human respiration. The device is mounted on a 125- μm polyimide film for stable measurements. (b) Monitoring human respiration by the sensor. The used sensor is indicated by the dashed square in (a).

Monitoring water evaporation on skin. Figure 5(a) shows the measurement system for monitoring water evaporation on skin. In order to detect water evaporation on skin easily, a NC-film humidity sensor is set in a plastic case (size: 36 mm×36 mm×14 mm). When human skin covers over the plastic case without touching a NC film (distance between a hand and a sensor: 9 mm), water evaporates on the skin and diffuses into the case. The sensor detects the increase of humidity in the plastic case due to the diffused water. Figure 5(b) shows the detection of water evaporation from a human hand. As a control experiment, the case is alternately covered with a bare hand and a hand with a rubber glove. The sensor responds only when the bare hand covers the case; and therefore, the sensor detects the sweat evaporated from the hand. In Figure 5(c), real-time detection of water evaporation is demonstrated. With around 2-s intervals, the plastic case is covered by a bare hand. The sensor detects increase of humidity in the plastic case cyclically.

A previous report showed that a wearable humidity sensor was directly attached on a fingertip to monitor sweat.⁷ On the other hand, in this study, the NC-based sensor detects sweat evaporation without contacting skin. Since nano-scale materials might translocate through human skin²⁷, remote detection of water evaporation on skin is a more non-invasive method. Note that there are two processes of water evaporation on human skin: active secretion from sweat glands (perspiration) and passive diffusion of water through epidermis (trans-epidermal water loss).⁴⁴ Perspiration is related to physiological stress and the amount of trans-epidermal water loss depends on skin condition. The NC-based sensor has a potential to monitor these physiological and physical conditions of human in real time.

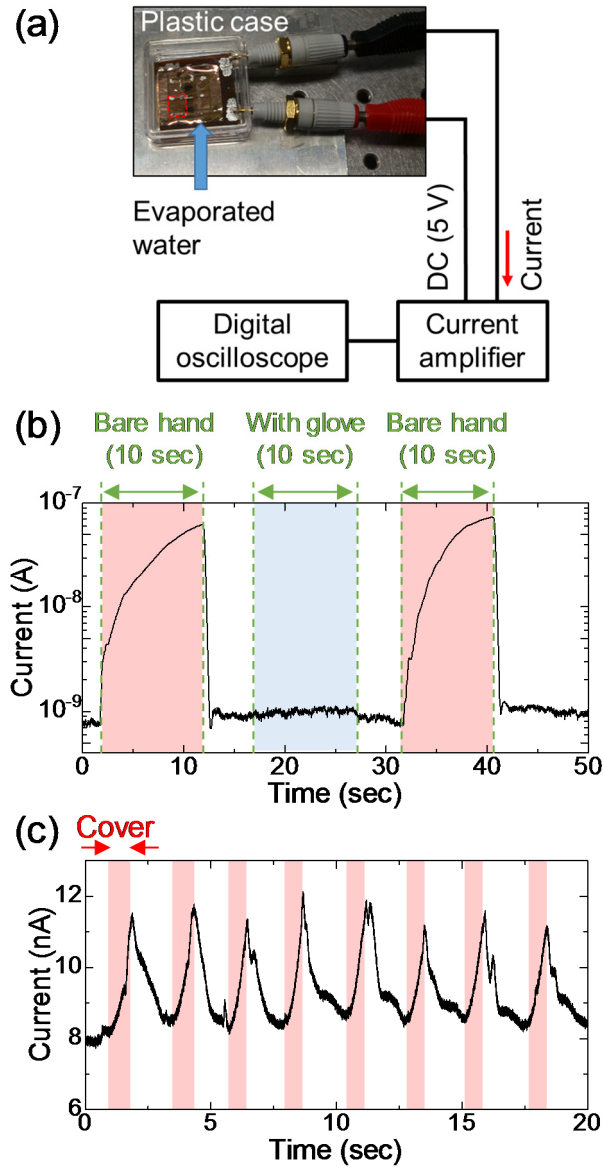


Figure 5. (a) Measurement system for monitoring water evaporation on human skin. The device indicated by the dashed square is wired to banana-type terminals. (b) Monitoring water evaporation from a bare hand. (c) Real-time detection of water evaporation from a hand. Colored periods are the time when the case is covered by a bare hand.

CONCLUSIONS

We have developed a fast-response and flexible NC-based humidity sensor for human health monitoring. An all-inorganic Si NC film was used as a humidity-sensitive material. The current readout of the sensor changed by five orders of magnitude in the relative humidity range between 8 and 83 %. The sensor exhibited fast response to humidity change with the response/recovery time of 40 ms at 3 Hz. We demonstrated real-time monitoring of human respiration and water evaporation on skin by using the sensor. The fast-response and flexible NC-based humidity sensor can be suitable for personal health monitoring as well as environmental monitoring.

ASSOCIATED CONTENT

Supporting information

The Supporting Information is available free of charge on the ACS Publications website at DOI:***. Current-voltage characteristics of a bent NC-based humidity sensor (Figure S-1). Relative humidity dependence of current through interdigitated electrodes on a polyimide film without a Si-NC film (Figure S-2). Responses of a NC-based humidity sensor to chopped humid N₂ (Figure S-3). Response and recovery time of a NC-based humidity sensor when relative humidity changes between 20 % and >95 % (Figure S-4). Videos of demonstration of monitoring human respiration and water evaporation from a hand.

AUTHOR INFORMATION

Corresponding Author

*E-mail: kano@eedept.kobe-u.ac.jp (S.K)

Notes

The authors declare no competing financial interest.

ACKNOWLEDGMENTS

This work was partly supported by JSPS KAKENHI Grant Number 16H03828, Visegrad Group (V4)-Japan Joint Research Project on Advanced Materials “NaMSeN”, Hyogo Science and Technology Association, and the Kyoto Technoscience Center.

REFERENCES

- (1) Chen, Z.; Lu, C. Humidity Sensors: A Review of Materials and Mechanisms. *Sens. Lett.* **2005**, *3*, 274–295.
- (2) Yang, Y. C.; Pan, F.; Liu, Q.; Liu, M.; Zeng, F. Fully Room-Temperature-Fabricated Nonvolatile Resistive Memory for Ultrafast and High-Density Memory Application. *Nano Lett.* **2009**, *9*, 1636–1643.
- (3) Blank, T. A.; Eksperiandova, L. P.; Belikov, K. N. Recent Trends of Ceramic Humidity Sensors Development: A Review. *Sensors Actuators, B Chem.* **2016**, *228*, 416–442.
- (4) Matzeu, G.; Florea, L.; Diamond, D. Advances in Wearable Chemical Sensor Design for Monitoring Biological Fluids. *Sensors Actuators, B Chem.* **2015**, *211*, 403–418.
- (5) Trung, T. Q.; Lee, N. E. Flexible and Stretchable Physical Sensor Integrated Platforms for Wearable Human-Activity Monitoring and Personal Healthcare. *Adv. Mater.* **2016**, *28*, 4338–4372.
- (6) Mogera, U.; Sagade, A. a; George, S. J.; Kulkarni, G. U. Ultrafast Response Humidity Sensor Using Supramolecular Nanofibre and Its Application in Monitoring Breath Humidity and Flow. *Sci. Rep.* **2014**, *4*, 4103.
- (7) Miyoshi, Y.; Miyajima, K.; Saito, H.; Kudo, H.; Takeuchi, T.; Karube, I.; Mitsubayashi, K. Flexible Humidity Sensor in a Sandwich Configuration with a Hydrophilic Porous Membrane. *Sensors Actuators, B Chem.* **2009**, *142*, 28–32.

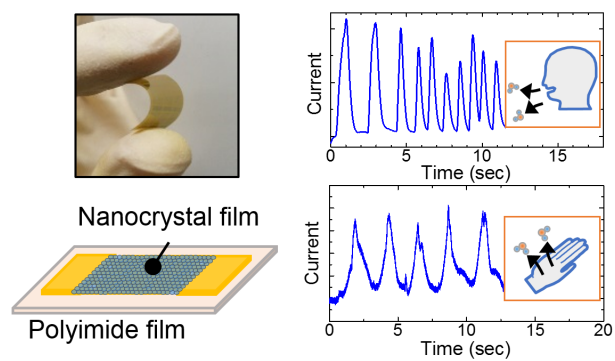
- (8) Khan, Y.; Ostfeld, A. E.; Lochner, C. M.; Pierre, A.; Arias, A. C. Monitoring of Vital Signs with Flexible and Wearable Medical Devices. *Adv. Mater.* **2016**, *28*, 4373–4395.
- (9) Su, P. G.; Wang, C. S. Novel Flexible Resistive-Type Humidity Sensor. *Sensors Actuators, B Chem.* **2007**, *123*, 1071–1076.
- (10) Su, P. G.; Tseng, J. Y.; Huang, Y. C.; Pan, H. H.; Li, P. C. Novel Fully Transparent and Flexible Humidity Sensor. *Sensors Actuators, B Chem.* **2009**, *137*, 496–500.
- (11) Sreeprasad, T. S.; Rodriguez, A. a; Colston, J.; Graham, A.; Pallem, V.; Berry, V. Electron-Tunneling Modulation in Percolating-Network of Graphene Quantum Dots : Fabrication , Phenomenological Understanding , and Humidity / Pressure Sensing Applications. *Nano Lett.* **2013**, *13*, 1757–1763.
- (12) Yan, Y.; Warren, S. C.; Fuller, P.; Grzybowski, B. A. Chemoelectronic Circuits Based on Metal Nanoparticles. *Nat. Nanotechnol.* **2016**, *11*, 603–608.
- (13) Borini, S.; White, R.; Wei, D.; Astley, M.; Haque, S.; Spigone, E.; Harris, N.; Kivioja, J.; Ryhänen, T. Ultrafast Graphene Oxide Humidity Sensors. *ACS Nano* **2013**, *7*, 11166–11173.
- (14) Jalkanen, T.; Mäkilä, E.; Määttänen, A.; Tuura, J.; Kaasalainen, M.; Lehto, V. P.; Ihalainen, P.; Peltonen, J.; Salonen, J. Porous Silicon Micro- and Nanoparticles for Printed Humidity Sensors. *Appl. Phys. Lett.* **2012**, *101*, 21–25.
- (15) Ozdemir, S.; Gole, J. L. The Potential of Porous Silicon Gas Sensors. *Curr. Opin. Solid State Mater. Sci.* **2007**, *11*, 92–100.
- (16) Smith, A. D.; Elgammal, K.; Niklaus, F.; Delin, A.; Fischer, A. C.; Vaziri, S.; Forsberg, F.; Rålander, M.; Hugosson, H.; Bergqvist, L.; *et al.* Resistive Graphene

- Humidity Sensors with Rapid and Direct Electrical Readout. *Nanoscale* **2015**, *7*, 19099–19109.
- (17) Bi, H.; Yin, K.; Xie, X.; Ji, J.; Wan, S.; Sun, L.; Terrones, M.; Dresselhaus, M. S. Ultrahigh Humidity Sensitivity of Graphene Oxide. *Sci. Rep.* **2013**, *3*, 2714.
- (18) Zhang, D.; Tong, J.; Xia, B.; Xue, Q. Ultrahigh Performance Humidity Sensor Based on Layer-by-Layer Self-Assembly of Graphene Oxide/polyelectrolyte Nanocomposite Film. *Sensors Actuators, B Chem.* **2014**, *203*, 263–270.
- (19) Segev-bar, M.; Haick, H. Flexible Sensors Based on Nanoparticles. *ACS Nano* **2016**, *7*, 8366–8378.
- (20) Sakai, G.; Baik, N. S.; Miura, N.; Yamazoe, N. Gas Sensing Properties of Tin Oxide Thin Films Fabricated from Hydrothermally Treated Nanoparticles. *Sensors Actuators B Chem.* **2001**, *77*, 116–121.
- (21) Joseph, Y.; Guse, B.; Yasuda, A.; Vossmeier, T. Chemiresistor Coatings from Pt- and Au-Nanoparticle/nonanedithiol Films: Sensitivity to Gases and Solvent Vapors. *Sensors Actuators, B Chem.* **2004**, *98*, 188–195.
- (22) Nazzari, A. Y.; Qu, L.; Peng, X.; Xiao, M. Photoactivated CdSe Nanocrystals as Nanosensors for Gases. *Nano Lett.* **2003**, *3*, 819–822.
- (23) Liu, H.; Li, M.; Voznyy, O.; Hu, L.; Fu, Q.; Zhou, D.; Xia, Z.; Sargent, E. H.; Tang, J. Physically Flexible, Rapid-Response Gas Sensor Based on Colloidal Quantum Dot Solids. *Adv. Mater.* **2014**, *26*, 2718–2724.

- (24) Konvalina, G.; Haick, H. Effect of Humidity on Nanoparticle-Based Chemiresistors: A Comparison between Synthetic and Real-World Samples. *ACS Appl. Mater. Interfaces* **2012**, *4*, 317–325.
- (25) Dasog, M.; Kehrle, J.; Rieger, B.; Veinot, J. G. C. Silicon Nanocrystals and Silicon-Polymer Hybrids: Synthesis, Surface Engineering, and Applications. *Angew. Chemie - Int. Ed.* **2015**, 2322–2339.
- (26) Fujii, M.; Sugimoto, H.; Imakita, K. All-Inorganic Colloidal Silicon Nanocrystals—surface Modification by Boron and Phosphorus Co-Doping. *Nanotechnology* **2016**, *27*, 262001.
- (27) Reiss, P.; Carriere, M.; Lincheneau, C.; Vaure, L.; Tamang, S. Synthesis of Semiconductor Nanocrystals, Focusing on Nontoxic and Earth-Abundant Materials. *Chem. Rev.* **2016**, *116*, 10731–10819.
- (28) Sugimoto, H.; Fujii, M.; Imakita, K.; Hayashi, S.; Akamatsu, K. Phosphorus and Boron Codoped Colloidal Silicon Nanocrystals with Inorganic Atomic Ligands. *J. Phys. Chem. C* **2013**, *117*, 6807–6813.
- (29) Fujii, M.; Sugimoto, H.; Hasegawa, M.; Imakita, K. Silicon Nanocrystals with High Boron and Phosphorus Concentration Hydrophilic shell—Raman Scattering and X-Ray Photoelectron Spectroscopic Studies. *J. Appl. Phys.* **2014**, *115*, 84301.
- (30) Nomoto, K.; Sugimoto, H.; Breen, A.; Ceguerra, A. V.; Kanno, T.; Ringer, S. P.; Wurfl, I. P.; Conibeer, G. J.; Fujii, M. Atom Probe Tomography Analysis of Boron And/or Phosphorus Distribution in Doped Silicon Nanocrystals. *J. Phys. Chem. C* **2016**, *120*, 17845–17852.

- (31) Hori, Y.; Kano, S.; Sugimoto, H.; Imakita, K.; Fujii, M. Size-Dependence of Acceptor and Donor Levels of Boron and Phosphorus Codoped Colloidal Silicon Nanocrystals. *Nano Lett.* **2016**, *16*, 2615–2620.
- (32) Sugimoto, H.; Fujii, M.; Imakita, K.; Hayashi, S.; Akamatsu, K. All-Inorganic near-Infrared Luminescent Colloidal Silicon Nanocrystals: High Dispersibility in Polar Liquid by Phosphorus and Boron Codoping. *J. Phys. Chem. C* **2012**, *116*, 17969–17974.
- (33) Sasaki, M.; Kano, S.; Sugimoto, H.; Imakita, K.; Fujii, M. Surface Structure and Current Transport Property of Boron and Phosphorous Co-Doped Silicon Nanocrystals. *J. Phys. Chem. C* **2016**, *120*, 195–200.
- (34) Kano, S.; Sasaki, M.; Fujii, M. Combined Analysis of Energy Band Diagram and Equivalent Circuit on Nanocrystal Solid. *J. Appl. Phys.* **2016**, *119*, 215304.
- (35) Nečas, D.; Klapetek, P. Gwyddion: An Open-Source Software for SPM Data Analysis. *Cent. Eur. J. Phys.* **2012**, *10*, 181–188.
- (36) Agmon, N. The Grotthuss Mechanism. *Chem. Phys. Lett.* **1995**, *50*, 456–462.
- (37) Anderson, J. H.; Parks, G. A. The Electrical Conductivity of Silica Gel in the Presence of Adsorbed Water. *J. Phys. Chem.* **1968**, *72*, 3662–3668.
- (38) Seo, M. H.; Yang, H. H.; Choi, K. W.; Lee, J. S.; Yoon, J. B. A Simple Breathing Rate-Sensing Method Exploiting a Temporarily Condensed Water Layer Formed on an Oxidized Surface. *Appl. Phys. Lett.* **2015**, *106*, 53701-1–4.
- (39) Biju, K. P.; Jain, M. K. Effect of Polyethylene Glycol Additive in Sol on the Humidity Sensing Properties of a TiO₂ Thin Film. *Meas. Sci. Technol.* **2007**, *18*, 2991–2996.

- (40) Kuang, Q.; Lao, C.; Wang, Z. L.; Xie, Z.; Zheng, L. High-Sensitivity Humidity Sensor Based on a Single SnO₂ Nanowire. *J. Am. Chem. Soc.* **2007**, *129*, 6070–6071.
- (41) Fu, X. Q.; Wang, C.; Yu, H. C.; Wang, Y. G.; Wang, T. H. Fast Humidity Sensors Based on CeO₂ Nanowires. *Nanotechnology* **2007**, *18*, 145503.
- (42) Zampetti, E.; Pantalei, S.; Pecora, A.; Valletta, A.; Maiolo, L.; Minotti, A.; Macagnano, A.; Fortunato, G.; Bearzotti, A. Design and Optimization of an Ultra Thin Flexible Capacitive Humidity Sensor. *Sensors Actuators, B Chem.* **2009**, *143*, 302–307.
- (43) Guder, F.; Ainla, A.; Redston, J.; Mosadegh, B.; Glavan, A.; Martin, T. J.; Whitesides, G. M. Paper-Based Electrical Respiration Sensor. *Angew. Chemie - Int. Ed.* **2016**, *55*, 5727–5732.
- (44) Buettner, K. Diffusion of Water and Water Vapor through Human Skin. *J. Appl. Physiol.* **1953**, *6*, 229–242.



For Table of Contents Only